6. VOLCANICLASTIC FACIES AND SEQUENCES, LEG 129[1]

A.R.M. Salimullah[2]

ABSTRACT

Two sites (800 and 801) were drilled in the Pigafetta Basin and one site (802) in the East Mariana Basin during Ocean Drilling Program Leg 129. Thick (192–211 m) Cretaceous volcaniclastic sediments were encountered at all of the sites and an additional 222-m-thick Miocene-Pliocene volcaniclastic section was drilled at Site 802. On the basis of texture, structure, composition, and wireline log signature, these sediments can be divided into seven facies: debris-flow deposits, slumps, fluidized-flow deposits, grain-flow deposits, volcaniclastic turbidites, calcareous volcaniclastic turbidites, and pelagic sediments and bioclastic turbidites. Shallow-water debris in these volcaniclastic sediments includes red algae, ooids, oolitic grapestone, bivalves, and benthic foraminifers, which indicates that some of the source-area seamounts were at or near sea level. Calibration and interpretation of geophysical and geochemical logs with recovered cores and thin-section data has helped to characterize all of the facies types, to recognize slump facies more precisely, to determine the extent of the various facies, and to document the vertical sequences of facies in Hole 801B. This reveals the process continuum nature of resedimentation in the Pigafetta Basin, which is somewhat similar to that in siliciclastic basins. Moreover, apparently random distribution of these facies in the volcaniclastic succession as well as the presence of slumps, debris-flow deposits, and turbidites within thick (9–17 m) pelagic sediments (radiolarian-rich) indicates the high degree of tectonic instability of the Pigafetta Basin and the surrounding areas. This suggests that sedimentation was controlled largely by tectonics rather than by sediment supply.

INTRODUCTION

During Ocean Drilling Program (ODP) Leg 129, three sites were drilled in two mid-plate basins surrounded by seamounts in the west central Pacific Ocean. Sites 800 and 801 are located in the northwestern and central regions of the Pigafetta Basin and Site 802 is located in the East Mariana Basin (Fig. 1). The lithostratigraphy of the sites as summarized by the Shipboard Scientific Party (1990), is presented in Figure 2. Thick (211–227 m) Cretaceous volcaniclastic sediments were encountered at all three sites, and a thick (222 m) Miocene-Pliocene volcaniclastic section was also drilled at Site 802. These sediments account for about 53% of the cumulative thickness of the sedimentary intervals at the sites, although core recovery ranges from 17.5% to 29.5%.

The various sets of data that were used during this study include the following: visual core descriptions (VCD, shipboard sedimentologists); core photographs; thin-section/smear slide data; formation microscanner (FMS) images; dipmeter-microresistivity logs; CCI (calcium yield in decimal fraction) logs from geochemical combination string); CSI (silica yield in decimal fraction) logs from geochemical combination string.

The FMS and dipmeter-microresistivity logs are used in this study to provide information on the texture and structure of the sediments, whereas the geochemical logs are used to give information on their composition (Salimullah and Stow, in press, a and b). The FMS tool is a hybrid dipmeter tool (for details see Serra, 1989) which is capable of producing high-resolution borehole images from electrical conductivity measurements. The button current intensity (raw data points) is sampled every 2.5 mm (Serra, 1989) by the FMS. This contrasts markedly with most conventional downhole measurements (e.g., gamma-ray logging) that are averaged over 300–600 mm; hence the sampling rate of the FMS is 120 times larger than that of most other logging devices (C. M. Griffiths, pers. comm., 1990). The FMS has an imaging resolution on the order of a few millimeters in both vertical and azimuthal directions (Ekstrom et al., 1986). Sedimentary features as small as 1.2 cm can be resolved on the FMS images (Harker et al., 1990).

The main objectives of the study can be summarized as follows:

1. To delineate sediment facies within the volcaniclastic units of the sites in terms of texture, structure, and composition;

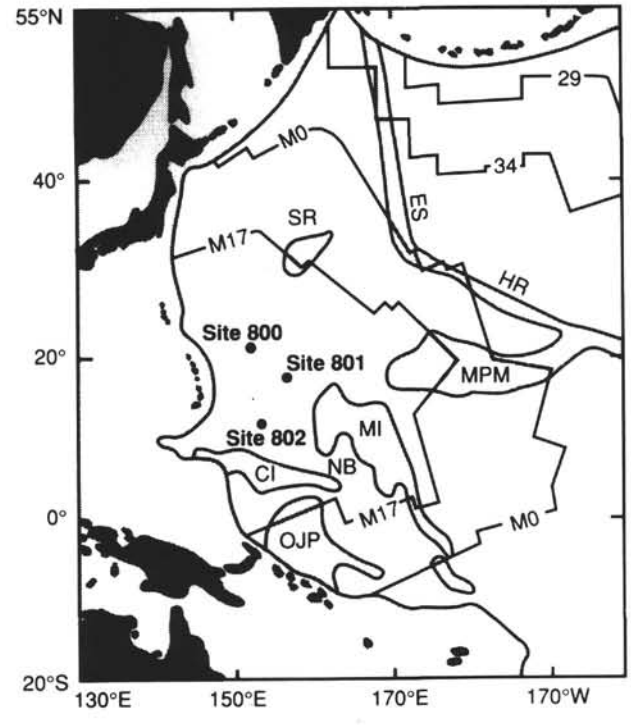

Figure 1. Location of Leg 129 Sites 800, 801, and 802. Jagged contours represent magnetic lineations and unshaded areas represent normal Pacific oceanic crust. Shaded areas represent volcanic edifices with thickened crustal sections, as well as younger areas beyond the Pacific subduction zones.

[1] Larson, R. L., Lancelot, Y., et al., 1992. *Proc. ODP, Sci. Results,* 129: College Station, TX (Ocean Drilling Program).

[2] Geology Department, The University of Southampton, Southampton SO9 5NH, United Kingdom.

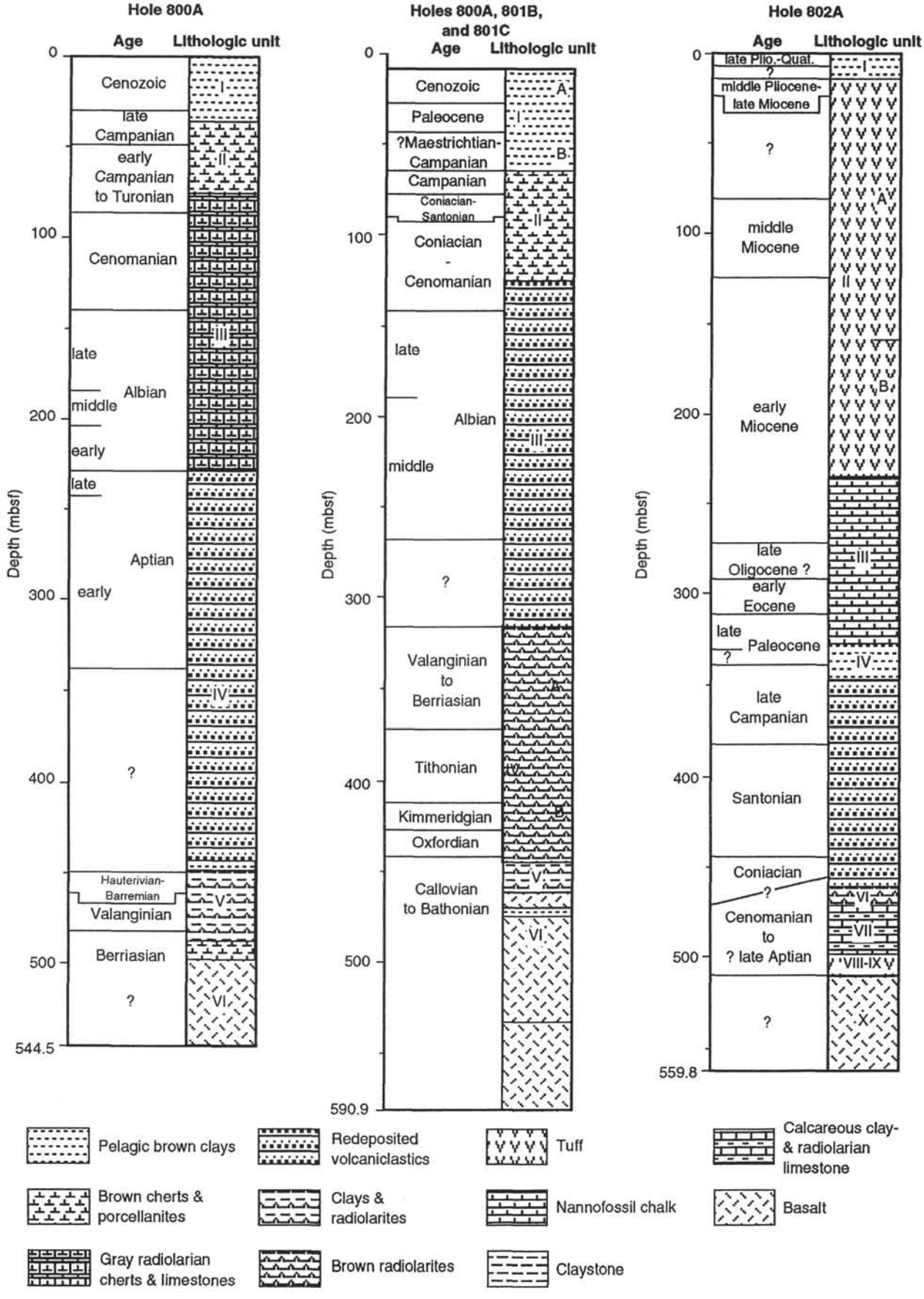

Figure 2. Summary of lithostratigraphy of Sites 800, 801, and 802.

2. To define each sediment facies in terms of the vertical evolution of the sedimentary features (texture and structure) to relate each facies to the specific process of deposition in a deep marine setting;

3. To delineate the presence and vertical extent of the facies using wireline logs in sections with poor core recovery in order to infer the range of thickness of various facies; and

4. To introduce if possible the concept of vertical sequence of resedimented facies of deposition of volcaniclastic sediments in mid-plate settings and its implication for regional tectonics.

FACIES

The volcaniclastic intervals at all three sites can be divided into seven facies in terms of texture, structure, and composition delineated from the recovered cores and also from wireline log signatures. The facies are debris-flow deposits, slumps, fluidized-flow deposits, grain-flow deposits, volcaniclastic turbidites, calcareous volcaniclastic turbidites, and pelagic sediments and bioclastic turbidites.

Debris-flow Deposits

Sediments in the debris-flow deposits facies are massive, poor to very poorly sorted, with random fabric and poor grading. The matrix ranges from clay size to medium sand size and is composed mainly of smectite/chloritic clays, glass, and calcite (replacive), with foraminifers, calcareous nannofossils, and radiolarians in places. Larger clasts are coarse sand to pebble size and are composed largely of mud containing clays and glass (mud clasts), and igneous rock fragments. These rip-up (mud) clasts are mainly subrounded to well rounded in definition, and some clasts contain laminae indicating a sedimentary parent rock. The conglomeratic debris-flow facies are present mainly in the Pigafetta Basin. On the contrary, subangular to angular (igneous/mud) clasts of the debris-flow breccia facies are seen largely in the East Mariana Basin. Orientation of the clasts varies from subhorizontal to subvertical, where the bedding plane is approximately horizontal. Beds are 70–150 cm thick and most of the bedding contacts are sharp. In terms of vertical grain-size evolution and the abundance of larger clasts, three types of debris-flow deposits can be recognized: (1) massive matrix supported debris-flow deposits (Fig. 3A) of dominantly matrix with some larger clasts in places; (2) massive clast supported debris-flow deposits (Fig. 3B) of dominantly larger clasts with some matrix; and (3) graded debris-flow deposits (Fig. 3C) that are graded matrix supported and inversely graded clast supported debris-flow deposits. The first two types are the most common at all three sites.

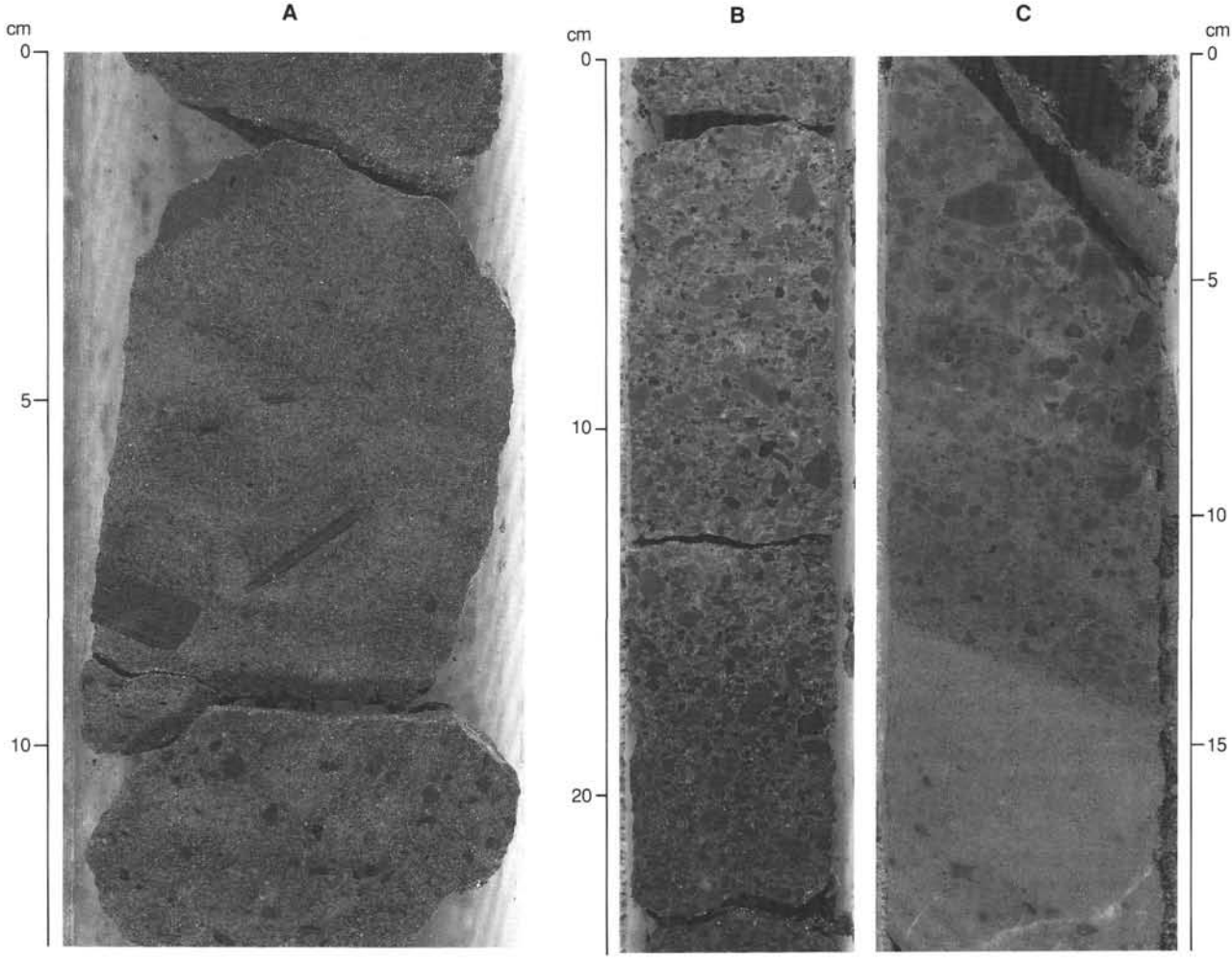

Figure 3. Core photographs of three types of debris-flow deposits. **A.** Matrix-supported debris-flow deposits (interval 129-801A-18R-1, 130–143 cm). **B.** Clast-supported debris-flow deposits (interval 129-800A-46R-2, 32–56 cm). **C.** Graded debris-flow deposits (interval 129-800A-46R-1, 48–63 cm). Note the presence of planar lamination in some of the larger clasts.

Slumps

There was little sediment recovery in the intervals thought to be related to sliding or slumping on the basis of their wireline log responses. Two possible intervals from which core was recovered are shown in Figure 4. They show sediment-mixing phenomena and recumbent folds accompanied by the water-escape features. However, FMS images reveal unique features of slumps, including microfolds and microfaults. The geometry and shape of the images provide evidence of recumbent slump folds (Fig. 5), accompanied by the probable water escape features, steeply inclined lamination, and possible chevron folding (Fig. 6). On the other hand, where images on the pads have a different texture or aspect or display a loss of continuity between the two sides, they may indicate faulting (Serra, 1989). Small depth shifts between similar features on each pad can indicate a microfault. The faults make a steep angle with the stratification and appear to show normal displacement. Moreover, the images show that the sedimentary features resembling turbidites (e.g., graded bedding, lamination) and pelagic sediments (horizontal stratification) are still distinct within some slumped intervals. This suggests coherent sliding/slumping of locally derived turbidite packages.

A continuous change of dip, both in magnitude and azimuth, indicates recumbent folding (Serra, 1985, 1989), which is present in various intervals of Hole 801B. Moreover, a relatively higher degree of apparent dip is observed in some intervals (e.g., 42° at about 252 meter below seafloor [mbsf] in Hole 801B, Fig. 13). CSI logs (Fig. 12) reveal that the slumping probably also affects some siliceous sediments (clayey radiolarites/radiolarian claystones) within the volcaniclastic interval, because the log readings correspond to the underlying lithostratigraphic unit, which is radiolarian rich (brown radiolarite, Fig. 2, Site 801).

Fluidized-flow Deposits

The sediments of this facies are mainly medium to fine sand size with a small proportion of very fine sand- to silt-size matrix. Grains are well to very well sorted and subrounded to angular. Beds are 70–90 cm thick and the bedding contacts are indistinct. They show no grading and contain many water-escape structures, among which vertical fluid-escape pipes and flame features are dominant. Some beds are accompanied by a load striation(s) at the base and convoluted laminae at the top. The sediments are composed largely of glass, igneous rock fragments, pyroxene, and calcite (replacive) with a minor proportion of radiolarians, smectite, and red algae in places. Based on the occurrence of the fluid-escape features, three types of beds can be recognized:

1. Fluidized-flow beds with vertical pipes (Fig. 7A) in which except for pipes no other features are visible. The pipes are closely spaced and are typically 2–7 cm long. Grain-size differences between the piped and unpiped sediments is highly subtle.
2. Fluidized-flow beds with flamelike pipes (Fig. 7B) have flames 1 to 3 cm long and closely spaced.
3. Fluidized-flow beds with vertical pipes and convolute laminae (Fig. 7C) have relatively large (5–10 cm long) pipes that are present at the base, with convoluted laminae at the top of the beds.

Grain-flow Deposits

Sediments of the grain-flow deposits are dominantly fine to medium sand size, moderately sorted, and subrounded to angular in shape. There are some larger isolated clasts which are coarse sand to granule size and are oriented mainly parallel to the bedding. Beds are structureless and generally lack grading but in places show reverse grading. Beds are 30–70 cm thick and bedding contacts are typically gradational. These sediments are composed largely of glass, igneous rock fragments, calcite (replacive), and radiolarians with a minor proportion of calcareous nannofossils, red algae, feldspar,

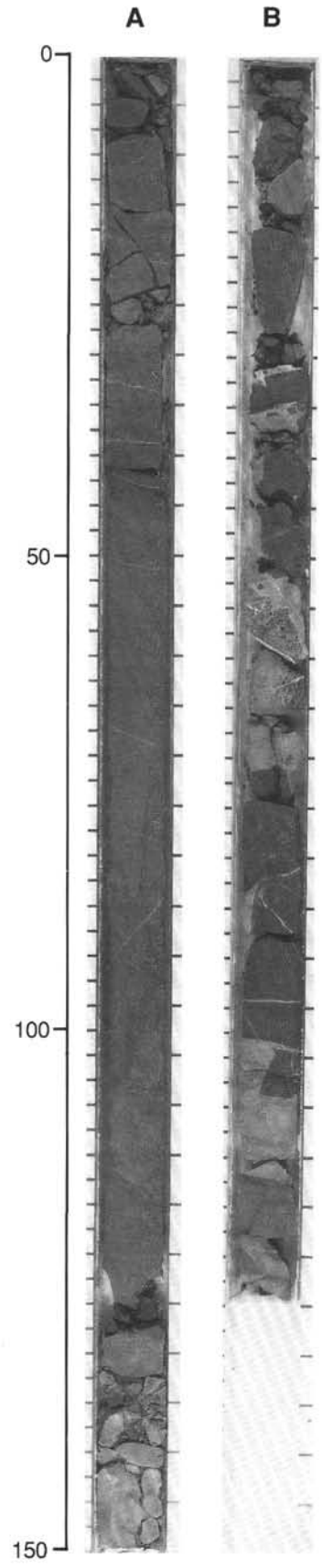

Figure 4. Core photographs of slump deposits. **A.** Recumbent microfolds and water-scape structures (pipes) (Section 129-800A-37R-1). **B.** Sediment mixing/amalgamated sediments (Section 129-800A-41R-1).

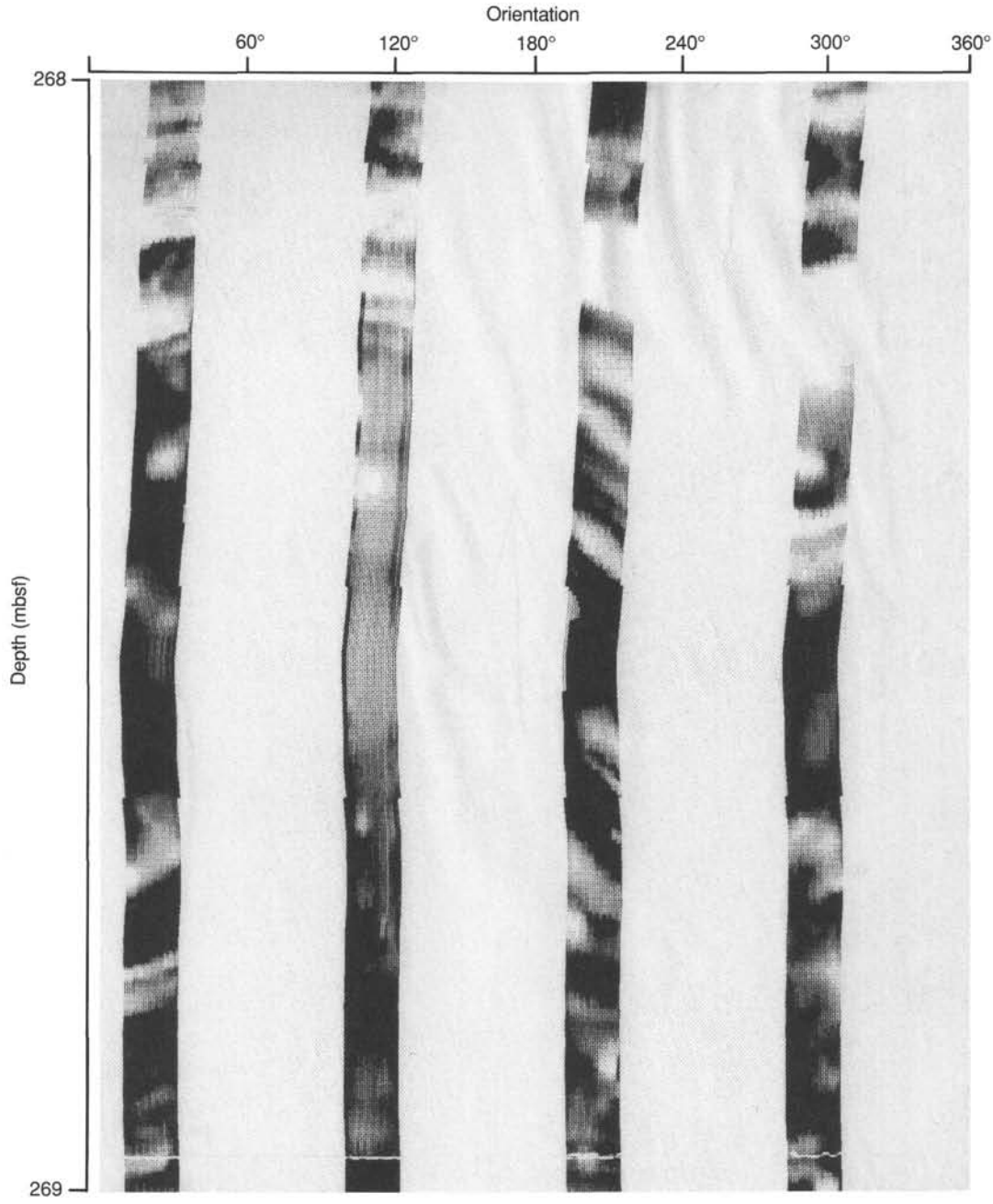

Figure 5. Characteristic four-pad FMS images (static pass) document the presence of recumbent folds (microfolds) and inclined beds in the nonrecovered cored interval from Hole 801B (268.0–279.0 mbsf).

and pyroxene. Based on sorting, two types of bed can be recognized: (1) grain-flow beds with coarser clasts (Fig. 8A) in which the clasts of mud and igneous rock fragments are scattered but oriented parallel to bedding plane; and (2) homogeneous grain-flow beds (Fig. 8B) that are well sorted with a few isolated clasts.

Volcaniclastic Turbidites

The sediments of the volcaniclastic turbidite facies are dominantly sand size with some mud and granule-size grains in places. The sediments are moderately to well sorted, angular to subrounded, and generally oriented parallel to bedding. Fining-upward trends in grain size in the beds are common. Common sedimentary structures are similar to coarse-, medium-, and fine-grained turbidite models (Bouma, 1962; Lowe, 1982; Stow, 1986) (Figs. 9A and 9B). The complete model sequence is rare. A continuum of coarse-, medium-, and fine-grained turbidite beds is also evident in some places. In addition to these classic bed sequences, two different type of beds are also observed and are locally dominant. One is characterized by fine-grained, thin bedding (2–10 cm), with enormous water-escape features (sediment mixing, fluidization/liquefaction channel; Fig. 9C). The other is characterized by fine-grained, moderately thick bedding (10–60 cm), with indistinct parallel laminae and bioturbation (Fig. 9D). The composition of the sediments varies locally, however,

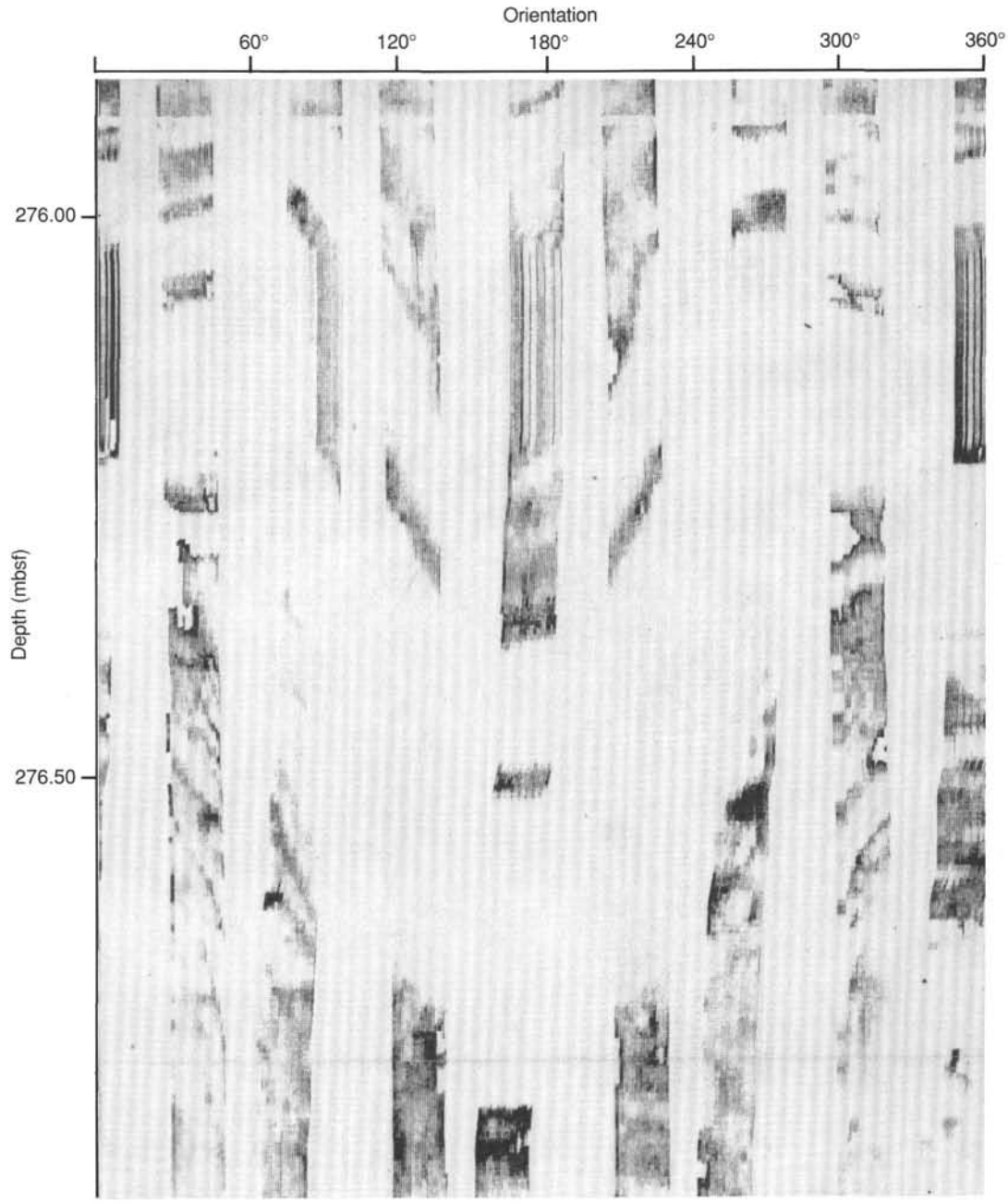

Figure 6. Four-pad FMS images (static merged pass) showing the presence of possible chevron folds in Hole 801B (275.87–276.87 mbsf).

the dominant components are glass, palagonite, igneous rock fragments, clays, and pyroxene with a minor proportion of zeolites, radiolarians, feldspars, and quartz.

Calcareous Volcaniclastic Turbidites

The texture and structure of the sediments of the calcareous volcaniclastic turbidite facies are similar to those of the volcaniclastic turbidite beds, although they differ in terms of composition as revealed in thin-section study. Turbidite beds that contain 10% or more primary calcareous material, including shallow-water flora, shallow- and deep-water fauna, and shallow-water nonbiogenic carbonates (excluding diagenetic/replacive carbonates), are termed calcareous turbidites. These sediments are composed of glass, palagonite, and igneous rock fragments with a variable proportion of red algae, ooids, oolitic grapestone clasts, bivalves, foraminifers, and calcareous nannofossils. Some beds contain as high as 60% calcareous red algae (Fig. 10A) at their base. Figure 10B shows the various calcareous components, including the well-rounded and well-preserved ooid clasts and partially eroded oolitic limestone (grapestone) clasts.

Pelagic Sediments and Bioclastic Turbidites

The sediments of pelagic sediment and bioclastic turbidite facies are clay size to fine sand size and are moderately sorted. Recovered cores (Fig. 11A) reveal alternate bands/bedding of very fine sand- to coarse-silt-size, brown-colored radiolarites (or clayey radiolarites), and clay- to medium-silt-size, gray-colored radiolarian claystones.

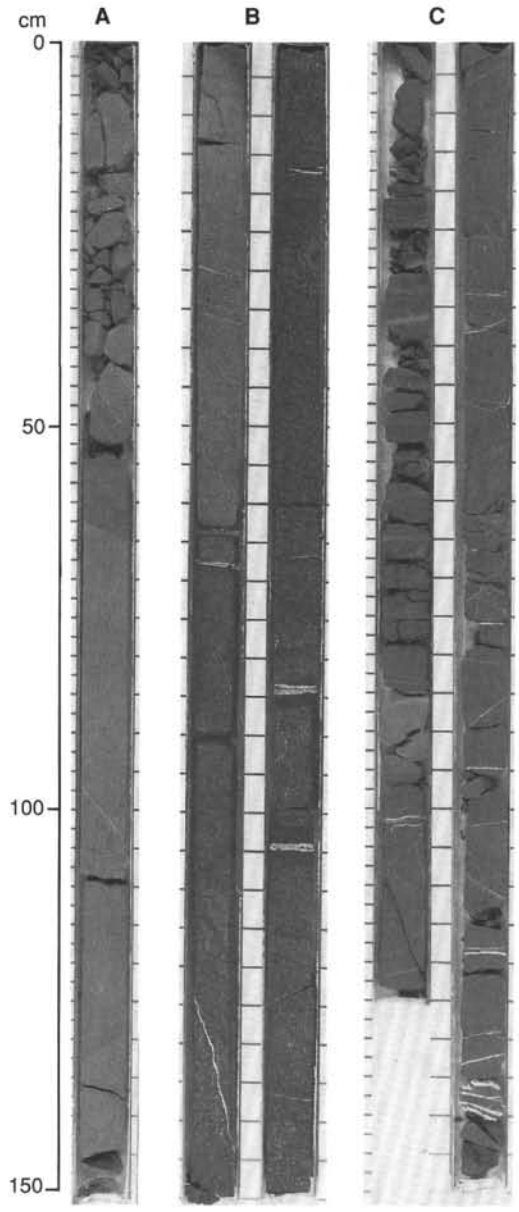

Figure 7. Core photographs of various fluidized-flow deposits. **A.** Beds with vertical pipes (Section 129-800A-45R-1). **B.** Beds with flamelike pipes (Sections 129-800A-33R-4 and 33R-5). **C.** Beds with vertical pipes (larger) and convolute laminae (Sections 129-800A-50R-1 and -50R-2).

There is some bioturbation that is mainly parallel to bedding and some indistinct flaser laminae in places. The sediments are composed dominantly of radiolarians and clays with a minor proportion of volcanic glass, barite, and zeolites. These characteristics are highly compatible with a pelagic origin (Jenkyns, 1986); however, FMS images (Fig. 11B) reveal that some beds are normally graded with an erosive lower bedding contact, which indicates the possible presence of bioclastic turbidites within a dominantly pelagic sequence. In addition, CSI log readings from these beds are similar to those of the underlying lithostratigraphic unit (Fig. 12), which contains radiolarian-rich sediments. The pelagic sediments and bioclastic turbidites facies described here occurs in thick continuous units (8.0–9.75 m) without volcaniclastic or other interbeds. There are also thin units (of a few centimeters) of pelagic sediments at the top of many volcaniclastic and calcareous volcaniclastic turbidites.

VERTICAL SEQUENCE OF FACIES

Average core recovery at the sites ranged between 17.5% and 29.5%, with the recovery in some volcaniclastic intervals being from 0% to 5%. This situation would have made it impossible to delineate any meaningful vertical sequences of facies. However, an extensive suite of wireline logs was successfully run through Hole 801B, including the entire interval within the volcaniclastic sediments, although the volcaniclastic intervals in the other holes were only partially covered by the wireline logging as a result of various obstacles. Hence, this part of the study will focus on Hole 801B. The wireline logs show the characteristic features for each of the volcaniclastic facies. The core:log correlation and interpretation of the individual logs in terms of characteristics of each facies and the combined use of the logs have greatly assisted in delineating the extent of the facies.

Core:Log Correlation Methodology

The FMS tool provides the high-resolution and continuous borehole coverage necessary to distinguish fine bedding, internal bed structures, and subtle changes in rock properties (Ekstrom et al., 1986). However, it is still crucial to integrate core data with openhole logs (Harker et al., 1990) to confidently establish lithological changes related to log trends. Thus, wireline log signatures including FMS images, dipmeter-microresistivity, and gamma-ray logs of the resedimented volcaniclastic facies have been documented (Salimullah and Stow, in press, a and b) and are used here to delineate vertical extent of the facies. The general core:log correlation and interpretation approach adopted is as follows:

1. Common sedimentary features (such as graded bedding, lamination, etc.) present within the various facies observed in recovered cores were correlated with the FMS images. These images were also compared with previously published FMS interpretation (e.g., Serra, 1986, 1989; Luthi, 1990). In this way we were able to build up a data base, for this suite of sediments, FMS images, and corresponding sedimentary interpretation.
2. In the intervals where there was no core recovery, the FMS images were compared with the data base developed in (1), hence allowing an interpretation of the nonrecovered section.
3. Dipmeter plots (angle and azimuth) were examined for each facies, especially noting the vertical evolution and distribution of dips. Different facies show different dipmeter patterns so it is possible to distinguish between facies (Salimullah and Stow, in press, a and b).
4. Microresistivity log readings were examined, especially to identify homogeneity and heterogeneity in terms of grain size for the massive structureless sands recognized from the cores and images.
5. The previous four steps were combined to delineate slumps, debris-flow deposits, grain-flow deposits, and turbidites and to delineate the extent of each facies within the hole.
6. Higher CCA log readings calibrated with the corresponding thin-section data were used to locate the calcareous volcaniclastic turbidites and to delineate their possible extent.
7. Higher CSI log readings calibrated with the thin-section data and compared with the readings corresponding to the underlying lithostratigraphic unit (brown radiolarite) were used to locate pelagic sediments and bioclastic (radiolarian) turbidites as well as their extent.

Vertical Sequence of Facies (Hole 801B)

In order to follow the aforementioned methodology for the interpretation of the wireline logs, a facies sequence of Hole 801B was

prepared (Fig. 13). The sequence shows that turbidites commenced as well as ended the volcaniclastic inputs at the site. It also reveals the absence of fluidized-flow facies at the site. The frequency of occurrence of facies sequences as well as their relative proportion of abundance (in percent) within the approximately 190-m-thick volcaniclastic unit, presented in Table 1, reveals that the turbidity currents were the dominant process for the volcaniclastic input.

The presence of all of the dominant resedimentation processes at the site indicates the process continuum nature that is somewhat similar to that observed in siliciclastic (continental marginal) settings. However, the random distribution of the facies may indicate that the regeneration and/or transformation of one process to another may not be a common phenomenon here, unlike in siliciclastic settings. The association of slumps with both turbidites and debris-flow deposits is nonlinear/random, which may indicate the high degree of tectonic instability of the site during sedimentation. Moreover, the presence of thick (9–17 m) radiolarian-rich sediments within the volcaniclastic unit indicates that Site 801 was cut off from volcaniclastic input and may imply that it was uplifted and/or shielded from the volcanic edifice(s), but it possibly lay above the carbonate compensation depth for a reasonable period of time.

Table 1. Summary data for the volcaniclastic facies sequences.

Facies type	Frequency of sequence	Thickness (m)	Abundance (%)
Volcaniclastic turbidites	10	3.75–20.0	54.60
Debris-flow deposits	5	3.75–9.75	16.66
Slumps	8	1.75–5.25	13.29
Pelagic sediments and bioclastic turbidites	2	8.00–9.75	9.21
Calcareous volcaniclastic turbidites	3	1.25–5.25	3.61
Grain-flow deposits	1	4.25	2.23

DISCUSSION

Sedimentary features and their vertical associations as well as vertical sequences of sedimentary structures typical of resedimented facies including turbidites, debris-flow deposits, and slumps are well documented in the volcaniclastic cores recovered during Leg 129. In the volcaniclastic sediments at Deep Sea Drilling Project (DSDP) Site 585, which lies north east of Site 802 in the East Mariana Basin, Whitman et al. (1986) focused their study mainly on the prevalent turbidites with only minor occurrence of debris-flow deposits. Slump blocks were also drilled at Site 585 (Moberly, Schlanger, et al., 1986). The same three resedimentation processes have been observed/described in volcanic island-arc settings (Cas, 1979; Cas and Wright, 1987; Fisher and Schmincke, 1984).

The maximum size of clasts (3–9 cm long) in some intervals of debris-flow facies generally indicates a weak to moderate flow strength. The range of thickness of the facies (3.75–9.75 m) at Site 801 indicates a more distal part of the flows and/or of localized flows with relatively weak strength. The presence of planar lamination in some mud clasts (rip-up clasts) indicates that the parent rocks were of sedimentary origin and were deposited by current-related processes. In addition, subrounded to well-rounded clasts in Sites 800 and 801 may indicate the relatively long period of sediment-transport in the Pigafetta Basin in comparison with that in the East Mariana Basin which largely contains subrounded to angular clasts, as reported from at Site 585 (Whitman et al., 1986).

Recumbent folds and sediment-mixing features accompanied by water-escape features in the partially recovered cores document the presence of slumps at Site 800, but the FMS images unequivocally show the additional classic features (recumbent and chevron folds associated with inclined beds and small-scale faults) in the nonrecovered intervals at Site 801. Moreover, the preservation of primary sedimentary features revealed with the FMS images in a number of intervals may indicate the presence of coherent sliding/slumping processes (Pickering et al., 1989). This is indicative of intrabasinal tectonic instability possibly induced by earthquake/volcanic tremors (Cas and Wright, 1987; Utada and Ito, 1989).

Whereas the volcaniclastic turbidites and the calcareous volcaniclastic turbidites display typical turbidite features (Salimullah and Stow, in press, a and b), and some of the beds interpreted as grain-flow and fluidized-flow deposits are very similar to those described by Middleton and Hampton (1973), other beds within these facies (e.g., those with subtle grading and indistinct lamination) perhaps indicate depositional processes transition between the end-members. It is also possible that the single long fluid escape pipes recognized may, in fact, represent the escape of primary magmatic fluids from a very proximal subaqueous pyroclastic flow-resedimented flow transition.

The presence of shallow-water fauna (e.g., bivalves and benthic foraminifers) and flora (e.g., red algae); shallow-water to lagoonal carbonates (e.g., ooids and oolitic grapestone); and glauconitic sands within various facies indicate that the source area seamounts were possibly and partly emerged at this time with large flank areas under relatively shallow-water depths (Haggerty and Silva, 1986; Bathrust 1975).

The integrated approach used in this paper, in which the interpretation of the wireline logs has been closely controlled with the core data, has been essential in completing the delineation of the vertical sequence of facies in Hole 801B. This vertical distribution of resedimented facies reveals that turbidity currents were the dominant process responsible for the deposition of the volcaniclastics. The presence of a series of slump deposits irrespective of bulk lithology (i.e., in both volcaniclastic-rich and radiolarian-rich sediments) and their association mostly with the debris-flow deposits indicate the high degree of tectonic instability during the volcaniclastic sedimentation. Moreover, the preservation of the sedimentary features (e.g., parallel bedding, graded bedding) revealed in the FMS images indicates the presence of coherent sliding phenomena (Pickering et al., 1989) indicative of intrabasinal tectonic instability leading to repeated earthquake/volcanic tremors.

Turbidity currents were presumably derived from sliding/slumping and debris-flow processes in an volcanic island-arc setting (Cas and Wright, 1987), so that the sedimentation was mainly controlled by volcano-tectonics rather than by sediment supply or sea-level effects.

CONCLUSIONS

From the combined study of cores, thin-sections, and wireline logs, the following conclusions about volcaniclastic sedimentation in the Pigafetta and the East Mariana basins, can be drawn:

1. Volcaniclastic sediments have been deposited by resedimentation processes, dominantly by turbidity currents.
2. The sediments in some intervals contain shallow-water calcareous debris transported by various processes that indicate that the source area seamounts and/or volcanic edifices were emerged possibly at or near sea level.
3. The presence of all the major resedimentation processes in these mid-plate Pacific basins is similar in many ways to those in siliciclastic basins (continental marginal basins) in terms of the process continuum nature.
4. The apparently random vertical distribution/association of these processes and facies at Site 801 suggests that the area was tectonically highly unstable during the period of volcaniclastic sedimentation.

5. The wireline log signatures of slumping, debris-flows, and turbidity currents in the thick (9–20 m) radiolarian-rich sediments within the volcaniclastic intervals further suggest that sedimentation was controlled largely by tectonics rather than by sediment supply or sea-level variation.

6. Further research may reveal more clearly the cause (origin) of this tectonism and its relation to regional volcanism.

ACKNOWLEDGMENTS

My sincere thanks to the Natural Environmental Research Council (NERC), U.K., for its financial support during participation in the cruise as well as post-cruise programs of Leg 129. I express my deep gratitude to the Geology Department of Southampton University and more specifically to my Ph.D. supervisor, Dr. D.A.V. Stow, for his support, suggestions, and corrections in preparing the manuscript as a whole. My gratitude is also expressed to the referees whose invaluable comments have refined the science of this manuscript.

REFERENCES

Bathurst, R.G.C., 1975. *Carbonate Sediments and Their Diagenesis* (2nd ed.): Amsterdam (Elsevier), 1–3.

Bouma, A. H., 1962. *Sedimentology of Some Flysch Deposits: A Graphic Approach to Facies Interpretation:* Amsterdam (Elsevier).

Cas, R., 1979. Mass flow arenites from a Paleozoic interarc basin, New South Wales, Australia: mode and environment of emplacement. *J. Sediment. Petrol.,* 49:29–44.

Cas, R.A.F., and Wright, J. V., 1987. *Volcanic Successions—Modern and Ancient:* Boston (Unwin and Hyman), 308–328.

Ekstrom, M. P., Dahan, C., Chen, M.-Y., Lloyd, P., and Rossi, D. J., 1987. Formation imaging with microelectrical scanning arrays. *Log Analyst,* 28:294–306.

Fisher, R. F., and Schmincke, H.-U., 1984. *Pyroclastic Rocks:* New York (Springer Verlag), 400–407.

Haggerty, J. A., and Silva, P., 1986. Ooids and shallow water debris in Aptian-Albian sediments from the East Mariana Basin, Deep Sea drilling Project Site 585: implications of deposition of ooids. *In* von Huene, R., Aubouin, J., et al., *Init. Repts. DSDP,* 84: Washington (U.S. Govt. Printing Office), 413–29.

Harker, S. D., et al., 1990. Methodology of formation micro-scanner image interpretation in Claymore and Scapa Fields (North Sea). *In* Hurst, A., Lovell, M. A., and Morton, A. C. (Eds.), *Geological Applications of Wireline Logs.* Geol. Soc. Spec. Publ. London, 48:13–23.

Jenkyns, H. C., 1986. Pelagic environments. *In* Reading, H. G. (Ed.), *Sedimentary Environments and facies:* Oxford (Blackwell Sci.), 343–362.

Lowe, D. R., 1982. Sediment gravity flows: II. Depositional models with special reference to the deposits of high density turbidity currents. *J. Sediment. Petrol.,* 52:279–97.

Luthi, S. M., 1990. Sedimentary structures of clastic rocks from electrical borehole images. *In* Hurst, A., Lovell, M. A., and Morton, A. C. (Eds.), *Geological Applications of Wireline Logs.* Geol. Soc. Spec. Publ. London, 48:3–10.

Middleton, G. V., and Hampton, M. A., 1973. Sediment gravity flows: mechanics of flow and deposition. *In* Middleton G. V., and Bouma A. H. (Eds.), *Turbidites and Deep Water Sedimentation.* Short Course Notes, Soc. Econ. Paleontol. Mineral., Pacific. Sect., 1–38.

Moberly, R., and Schlanger, S. O., et al., 1986. *Init. Repts. DSDP,* 89: Washington (U.S. Govt. Printing Office).

Pickering, K. T., Hiscott, R. N., and Hen, F. J., 1989. Sediment transport and deposition in the deep sea. *In Deep Marine Environments—Clastic Sedimentation and Tectonics:* Boston (Unwin Hyman), 13–38.

Salimullah, A.R.M., and Stow, D.A.V., in press a. Wireline log signatures of resedimented and volcanistic facies, ODP Leg 129, West Central Pacific. *In* Hurst, A., Griffiths, C. M., and Worthington, P. F. (Eds.), *Geological Applications of Wireline Logs, II.* Geol. Soc. Spec. Publ. London, 66.

————, in press b. Application of FMS images in poorly recovered coring intervals: examples from ODP Leg 129. *In* Hurst, A., Griffiths, C. M., and Worthington, P. F. (Eds.), *Geological Applications of Wireline Logs, II.* Geol. Soc. Spec. Publ. London, 66.

Serra, O., 1985. *Sedimentary Environments from Wireline Logs:* Houston (Schlumberger), 28–35, 160–168.

————, 1986. Information on sedimentary structures. *In Fundamentals of Well-Log Interpretation* (Vol. 2): *The Interpretation of Logging Data:* Amsterdam (Elsevier), 137–52.

————, 1989. *Formation Microscanner Image Interpretation:* Houston (Schlumberger Education Services), 16–96.

Shipboard Scientific Party, 1990. Site 800. *In* Lancelot, Y., Larson, R. L., et al., *Proc. ODP, Init. Repts.,* 129: College Station, TX (Ocean Drilling Program), 33–89.

————, 1990. Site 801. *In* Lancelot, Y., Larson, R. L., et al., *Proc. ODP, Init. Repts.,* 129: College Station, TX (Ocean Drilling Program), 90–170.

Stow, D.A.V., 1986. Deep clastic seas. *In* Reading, H. G. (Ed.), *Sedimentary Environments and Facies,* Oxford (Blackwell Sci.), 399–443.

Utada, M., and Ito, T., 1989. Sedimentary facies of the Mio-Pliocene volcanotectonic depressions along the volcanic front in northeast Honshu, Japan. *In* Tarra, A., and Masuda, F. (Eds.), *Sedimentary Facies in the Active Plate Margin:* Tokyo (Terra Sci.), Tokyo, 605–618.

Whitman, J. M., Baltuck, M., Haggerty, J. A., and Dean, W., 1986. Turbidite sedimentology and history of the East Mariana Basin. *Init. Repts. DSDP,* 89:365–388.

Date of initial receipt: 31 May 1991
Date of acceptance: 17 February 1992
Ms 129B-115

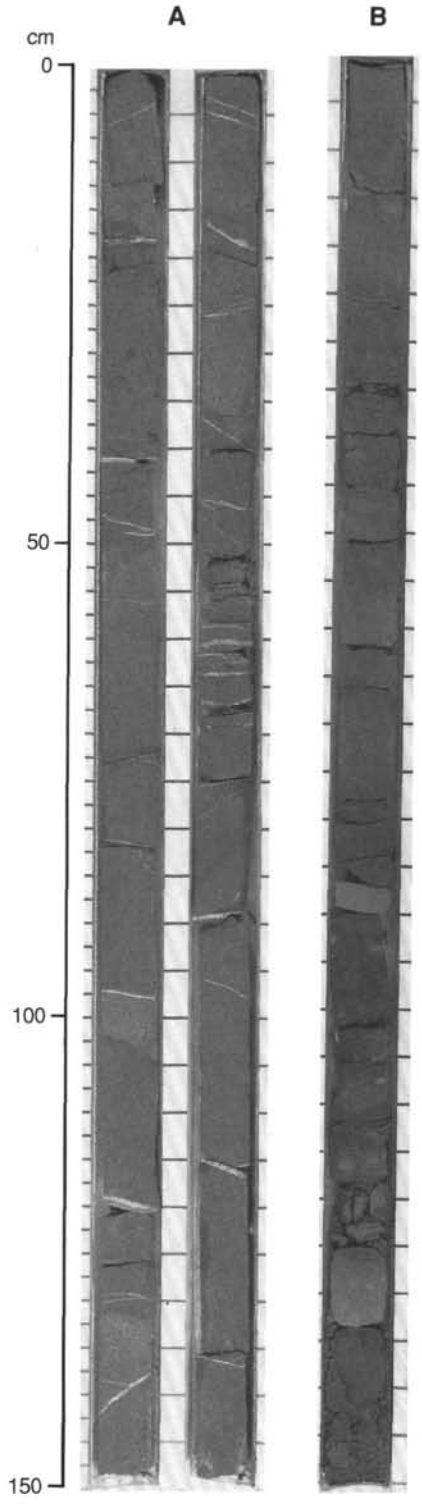

Figure 8. Core photographs of various bed of grain-flow deposits. **A.** Homogeneous beds (Sections 129-800A-48R-1 and -48R-2). **B.** Beds with some larger clasts in places (Section 129-801B-1R-4).

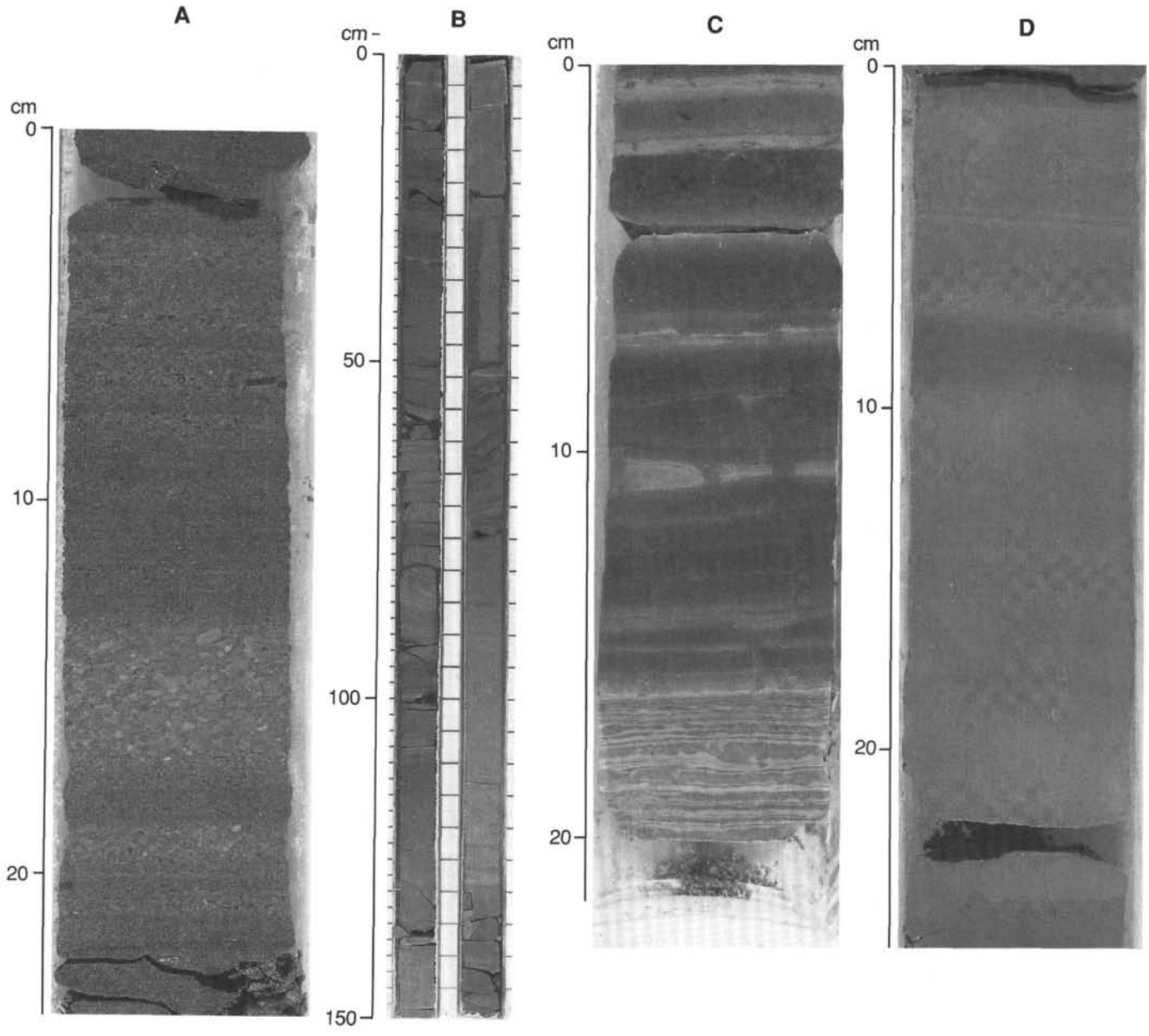

Figure 9. Core photographs of various volcaniclastic turbidite facies. **A.** Part of a coarse-grained turbidite bed (interval 129-802A-40R-2, 109–132 cm). **B.** Beds of medium-grained turbidites (Sections 129-800-31R-1 and 31R-2). **C.** Beds of fine-grained turbidites with water-escape structures (interval 129-801B-13R-1, 84–105). **D.** Beds of fine-grained turbidites with less-distinct laminations (interval 129-801B-8R-1, 14.5–37.0 cm).

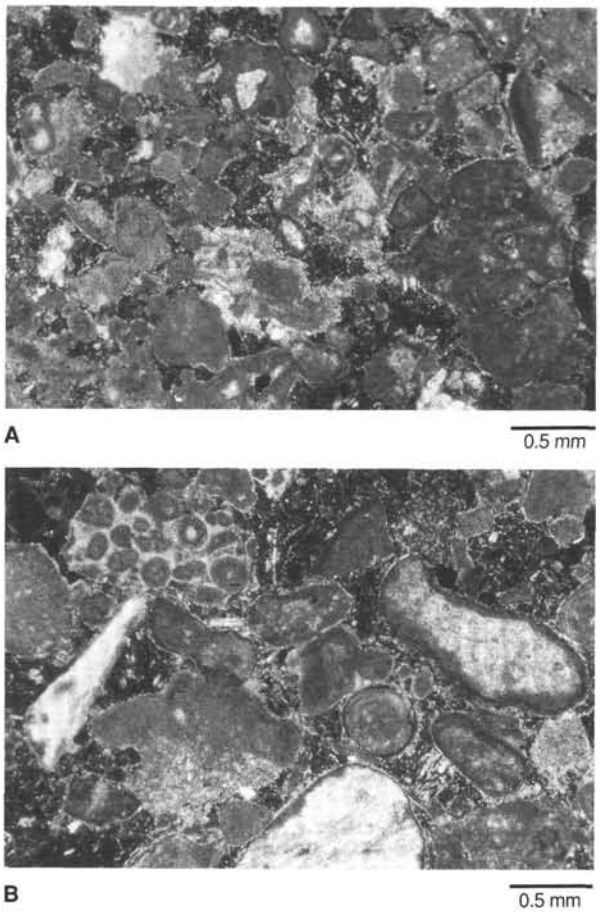

Figure 10. Photomicrographs revealing the calcareous composition of calcareous volcaniclastic turbidite facies. **A.** Large proportion of red algae with volcaniclasts and other shallow-water debris (crossed polars, Sample 129-800A-32R-1, 117–118 cm). **B.** Well-rounded ooids and subangular clast of oolitic grapestone (crossed polars, Sample 129-800A-32R-1, 117–118 cm).

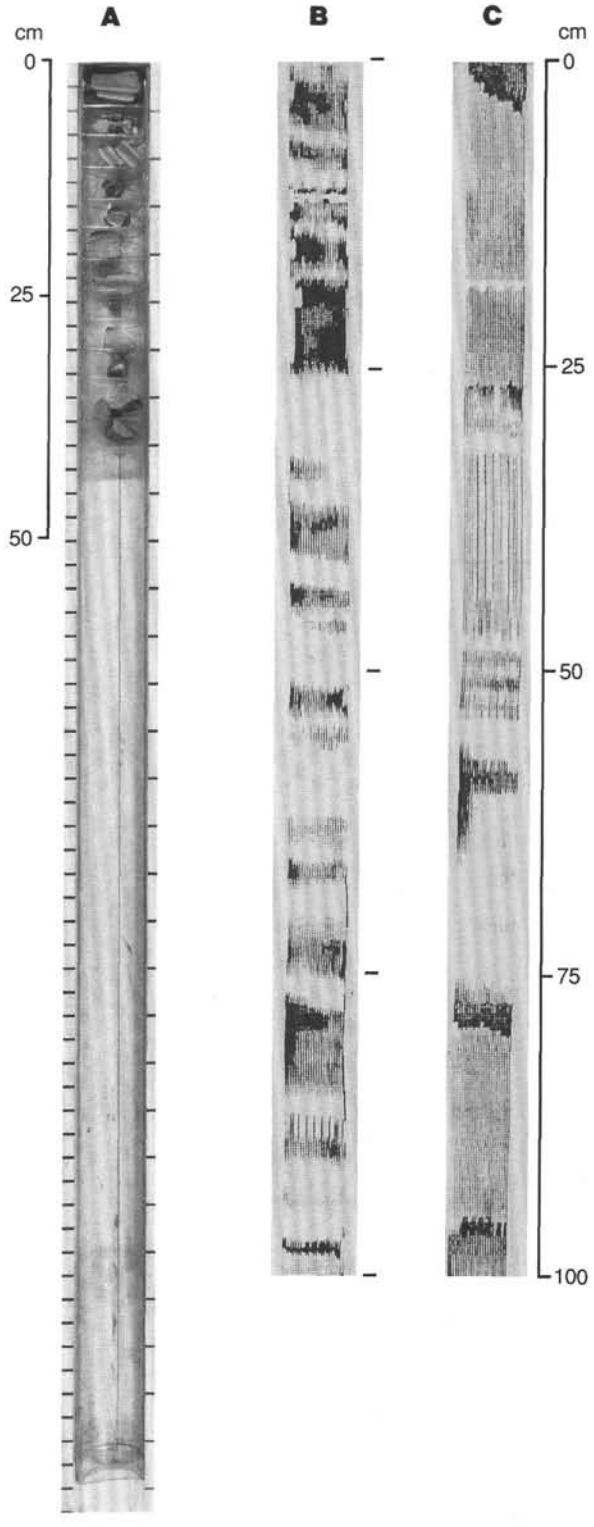

Figure 11. Pelagites and bioclastic turbidite facies. **A.** Core photograph of beds of pelagites (Section 129-801B-11R-1). **B.** FMS images of beds of pelagites (Hole 801B, 286.60–287.60 mbsf). **C.** FMS images of beds of bioclastic turbidites (Hole 801B, 177.50–178.50 mbsf). The FMS images can be compared to distinguish pelagites from bioclastic turbidites in terms of sedimentary features.

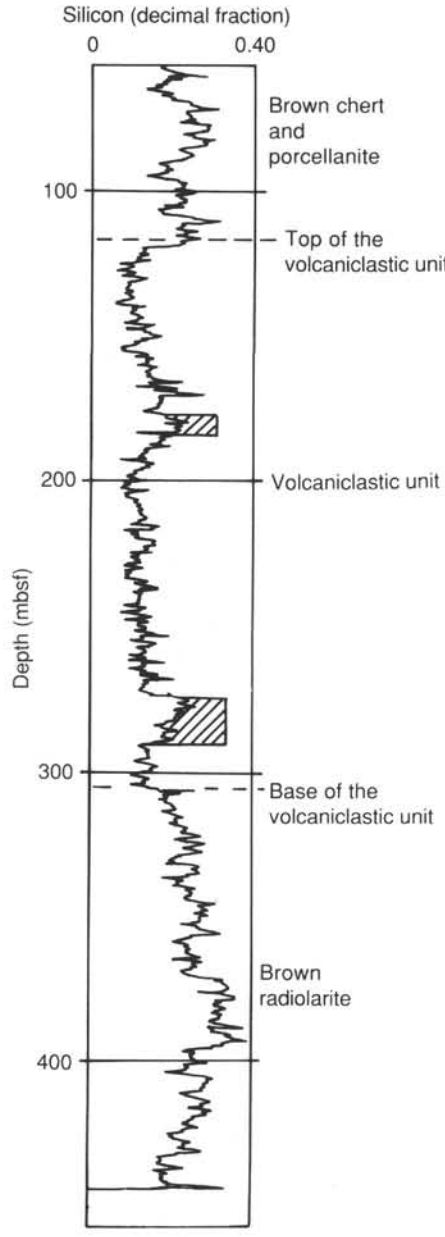

Figure 12. CSI logs showing the presence of radiolarian rich-sediments (hatched areas) within the volcaniclastic unit, Hole 801B. Note the log readings for the overlying (brown chert and porcellanites) and underlying (brown radiolarites) lithostratigraphic units.

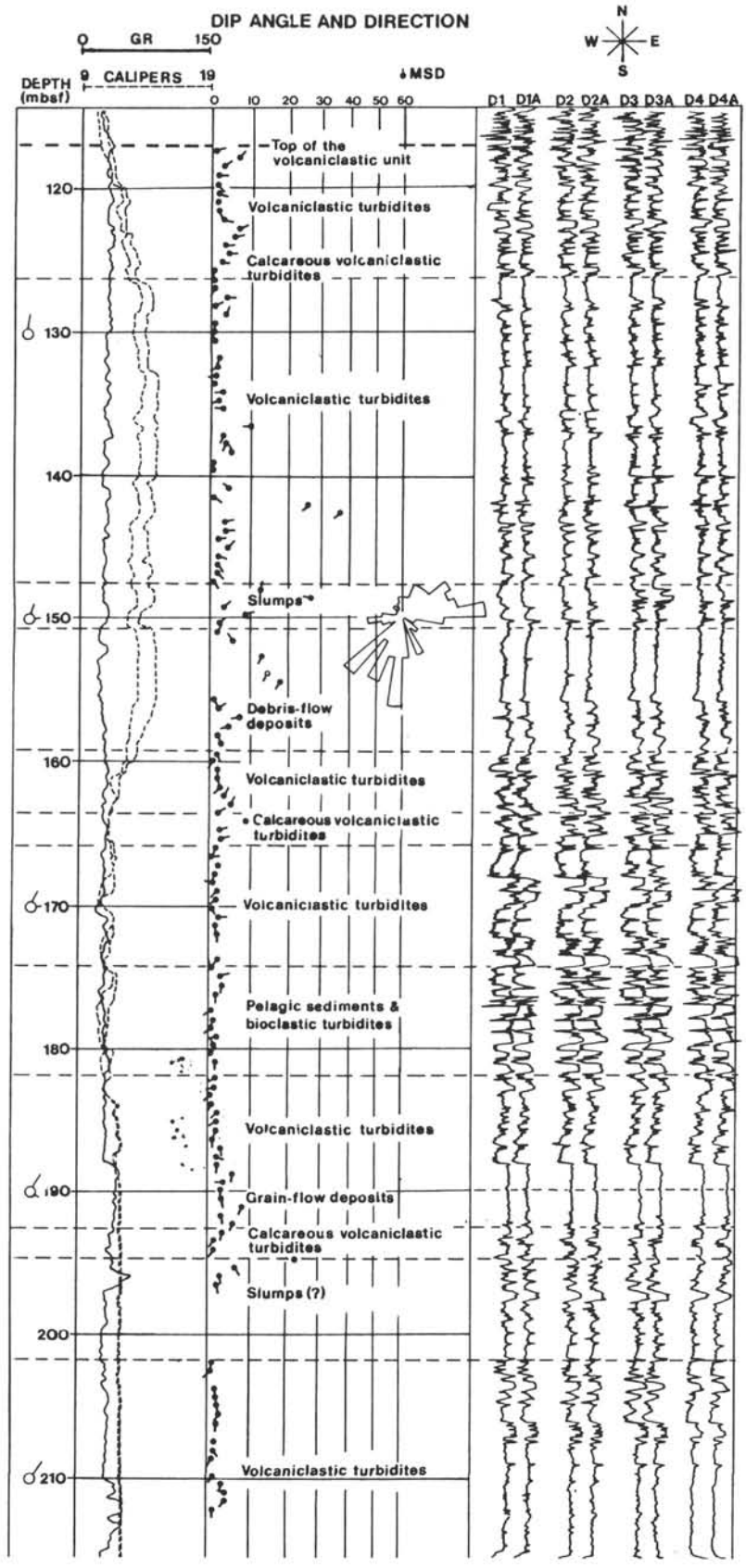

Figure 13. Vertical sequences of facies, Hole 801B. The dipmeter-microresistivity log sheets are used to show the vertical arrangement of facies, because they help to show the evolution of dips and azimuths for the various resedimented volcaniclastic facies.

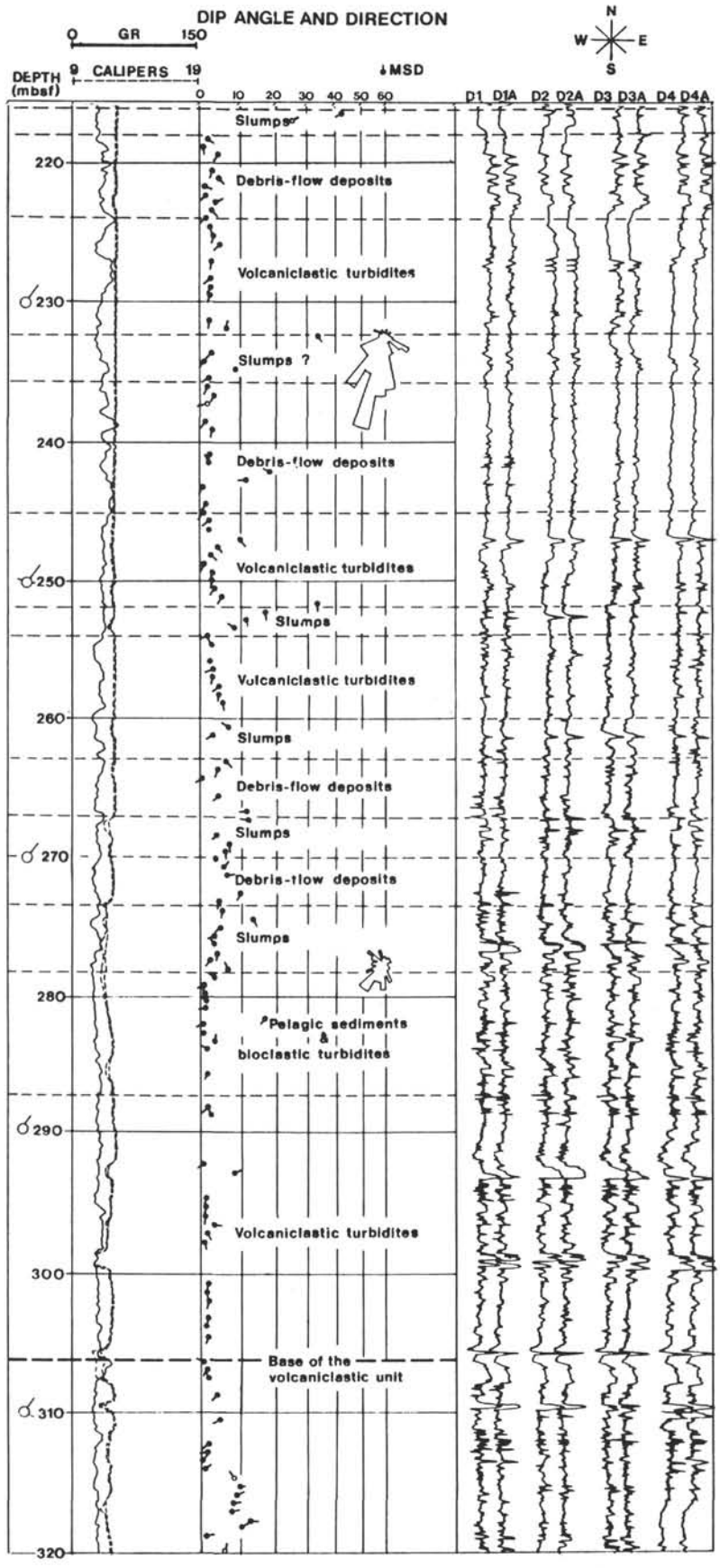

Figure 13 (continued).